

# Design of Metamaterial Based Multilayer Antenna for Navigation/WiFi/Satellite Applications

Aneri Pandya, Trushit Upadhyaya, and Killol Pandya\*

**Abstract**—Wireless communication plays a vital role in transmitting information from one point to another. Wireless devices have to be smart, intelligent, compact in size, and cost effective to meet the demand of wireless communication. A multi-layered, Split Ring Resonator (SRR), negative permeability material inspired antenna has been designed, analyzed, fabricated, and measured. The developed antenna resonates at 1.13 GHz, 2.47 GHz, and 2.74 GHz frequencies with gain of 3.73 dBi, 6.18 dBi, 1.35 dBi, and bandwidth of 2.10%, 2.81%, and 2.09%, respectively. The structure utilizes FR4 material as a substrate. The engineered model has applications in navigation, WiFi, and satellite communication applications.

## 1. INTRODUCTION

The growth of wireless communication demands a structural change in multiband antenna design to meet the present industry requirement. The requirement needs a smart, compact antenna that covers the application-oriented frequencies for navigation, WiFi, and satellite communication. In order to get the desired response, various feeding techniques could be utilized, viz., microstrip line feed, insert feed, and quarter-wave feed. The presented design utilizes a quarter-wave feeding technique to meet the maximum impedance matching requirement. The left-handed material helps to reduce the size of an antenna significantly and get the desired frequency bands for specific applications. Metamaterials are artificial materials that show negative permittivity and permeability for certain frequency spectrum [1–4]. Split Ring Resonator (SRR) is considered a fundamental block for metamaterials. The artificial metamaterials make themselves suitable for enhancing the electromagnetic properties of any microwave devices such as antennas. It also enhances filter performance with overall structure compactness and application-oriented frequency resonance [5, 6]. Dual-band microstrip antennas could be used for higher frequency performances [7]. Complementary Split Ring Resonator (CSRR) could also be an effective technique to enhance antenna performance [8].

The literature also exhibits a combination of microstrip slot and SRR which plays a significant role in designing a miniaturized antenna for dual-band performance [9]. The radiation characteristics and miniaturization techniques have been systematically covered in [10]. The researchers have also tested the SRR technique to get an adequate response from reconfigurable antennas [11]. The literature also covers a wide spectrum of miniaturization without the presence of SRR/CSRR; however, optimum size reduction may not be achievable [12, 13]. The present research work focuses on multiband metamaterial antennas targeting structure compactness, frequency selection, and antenna performance by introducing two-dimensional (2-D) metamaterial transmission lines and fractal geometries [14–18]. The metamaterials are artificial materials that could be utilized to receive particular electromagnetic properties that are not generally found in nature [19–21]. The combination of metamaterials and patches may lead to maximum power directivity and efficiency [22]. The dual bands could be achieved, and

---

*Received 1 October 2020, Accepted 1 December 2020, Scheduled 4 December 2020*

\* Corresponding author: Killol Pandya (killolpandya.ec@charusat.ac.in).

The authors are with the Charotar University of Science and Technology, India.

performance could be enhanced by adopting placement of a patch over another [23]. It is possible to improve return loss using a stacked metamaterial structure [24]. The conventional patch antenna has a limitation of directivity; however, metamaterial properties could be effectively utilized with conventional patch to make the radiation pattern more directional [25]. The negative permeability could be attained from  $S$ -parameters based on available literature [26]. Metamaterial-based multi-layer antennas have been proposed for navigation, WiFi, and satellite communications applications.

The presented paper is divided into several sections. The next section is reserved for claimed antenna geometry where details regarding antenna structure, shapes, and parameter dimensions have been discussed. Single SRR shape has also been touched upon. The subsequent section presents results and discussion. The response of proposed antenna regarding various key parameters such as return loss, gain, and electric field distribution is shown. This section also focuses on how adequate response could be obtained using a multi-layer structure. The last phase of the similar section gives information regarding the actual response of the presented antenna and how much variation is received between actual and simulated responses. The summary of the technical discussion is given in the conclusion section which is followed by references.

## 2. ANTENNA GEOMETRY

Antenna using microstrip patch is popular in general due to its light weight, low cost, and simple fabrication techniques. However, in order to improve its efficiency, bandwidth, size, and directivity, the researcher needs to enhance trade-offs between antenna structure and its designing parameters. For an instance, the bandwidth of an antenna could be improved significantly using a thicker substrate which may increase the overall power loss. Microstrip patch antenna generally has a significant unwanted radiation in vertical direction with reference to patch plane [27]. As a remedy for the discussed points, a metamaterial based antenna is proposed. Metamaterial is a negative refractive indexed artificial material. It is designed to get miniaturized antenna with desirable gain and bandwidth. The proposed antenna has six SRRs which are introduced to create negative refractive indexed material.

The proposed antenna has been designed using a commercially available substrate FR4 which has relative permittivity 4.4 and dielectric loss tangent 0.001. FR4 is a lossy material in comparison with Rogers laminates; however, carefully designed parameters have been chosen to get the desired response. The presented antenna structure contains three layers. The bottom layer is an FR4 substrate having the standard height of 1.56 mm. The primary patch has been created on the top of the first layer. There is an air gap of 3 mm which is retained just above the bottom substrate layer. The six SRRs have been placed on the top of the air gap. The top layer has equivalent dimensions to that of bottom layer. The secondary patch has been developed on the top substrate layer. Figure 1 shows cross section view of proposed antenna. As shown in figure, to mechanically accommodate the air gap between two substrates, insulating support is required for stability. The Top view of mentioned multilayer structure is systematically shown in Figure 2 using iterations. The first iteration (Figure 2(a)) includes a primary patch on the lower substrate layer. The second iteration covers slot introduction in the primary patch as shown in Figure 2(b). Split ring resonators are shown in Figure 2(c) using the third iteration. The top view of the multilayer structure is shown in Figure 2(d) using the forth iteration. In the result and discussion section, the response after each iteration is covered for better understanding. Figure 3 focuses on the proposed design of SRR. All necessary dimensions are marked and presented in Table 1.

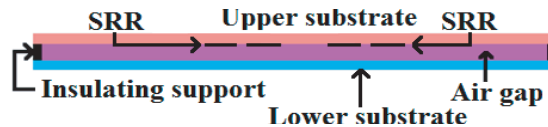


**Figure 1.** Cross section of proposed antenna.

Figure 4 shows the bird eye view of the proposed antenna. The secondary patch on top of the upper substrate is visible. All necessary dimensions are marked within the figures.

The proposed antenna model has been fabricated using PCB machine. The secondary patch on the

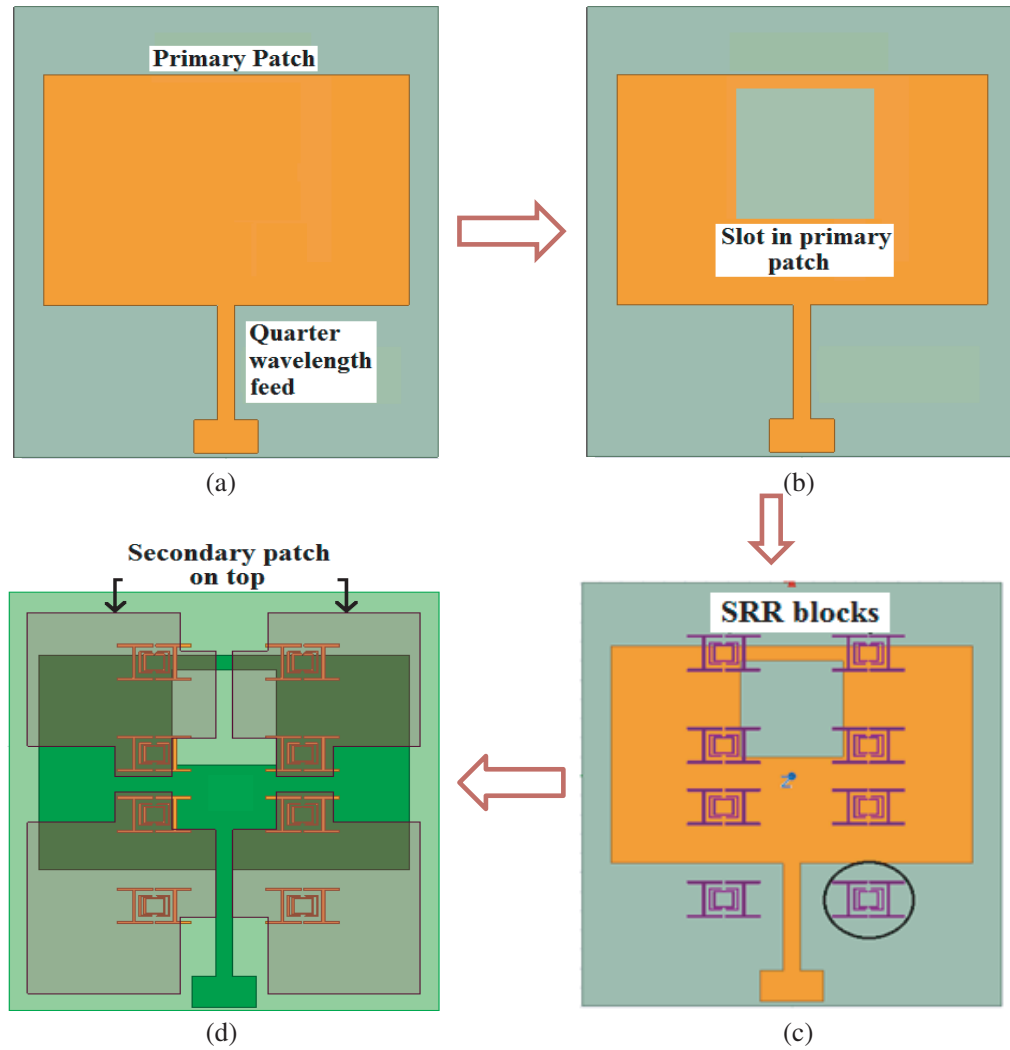


**Figure 2.** Systematic development of proposed multilayer antenna design. (a) First iteration. (b) Second iteration. (d) Fourth iteration. (c) Third iteration.

top of upper substrate and ground plane are visible in Figures 5(a) and (b), respectively. Figure 5(c) depicts the bird eye view where air gap is visible.

Table 1 gives detailed dimensions of all parameters.

**Table 1.** Antenna dimensions.

Notation	Dimensions (mm)	Notation	Dimensions (mm)
$G1$	0.3	$W1$ (Upper patch)	20
$G2$	1.25	$h1$	1.56
$G3$	0.625	$h2$	3
$G4$	0.756	$h3$	1.56
$G5$	0.906	$W1$ (SRR)	0.63
$G6$	0.31	$G11$	4
$G7$	1.25	$S$	24

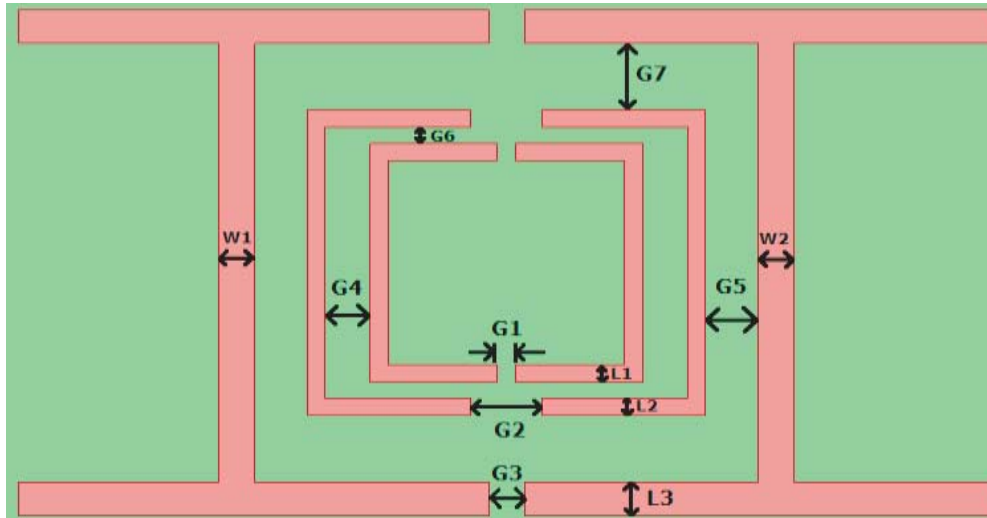


Figure 3. SRR design.

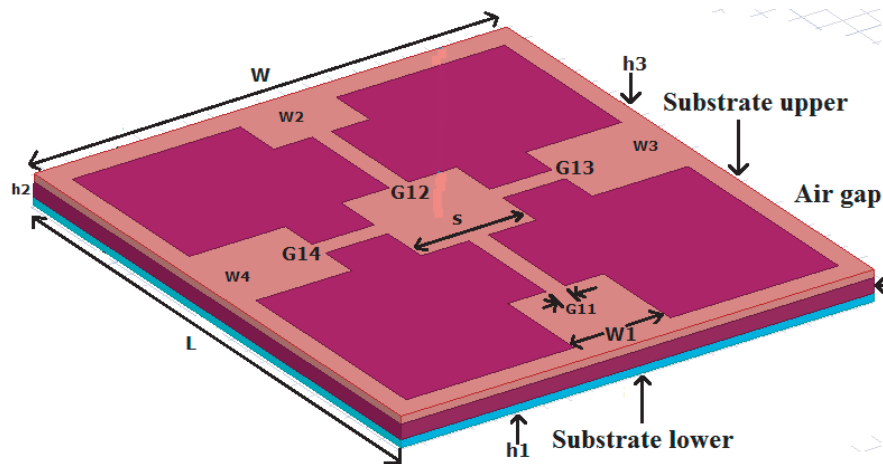


Figure 4. Bird eye view of proposed antenna.

### 3. RESULT AND DISCUSSIONS

The claimed antenna parameters have been analyzed using finite element method (FEM) based High Frequency Structure Simulator (HFSS). Figure 6 shows the comparison between simulated and measured return losses. The return loss measurement of an antenna is done using Keysight Vector Network Analyzer N9912A. The red color solid line represents the simulated result, and blue color dashed line represents the measured result. The measured result line is overlapping the simulated result line which claims the validation of simulated result.

Figure 7 shows the parametric study of return loss for various layers adopted in the presented antenna. The close observation shows that excellent return loss could be obtained using a multi-layer structure. Figure 8 depicts the gain vs frequency response. The maximum gain observed is 6.18 dBi at 2.47 GHz frequency, and peak gains of 3.73 dBi and 1.75 dBi are achieved at 1.13 GHz and 2.74 GHz, respectively.

Gain has a close correlation with the effective antenna size. To obtain an adequate gain with size constraints is a challenging task. Many researchers have worked on obtaining the acceptable gain with microwave component size restriction [28–34].

Figure 9 shows VSWR values for 1.13 GHz, 2.47 GHz, and 2.74 GHz frequencies which are 1.31,

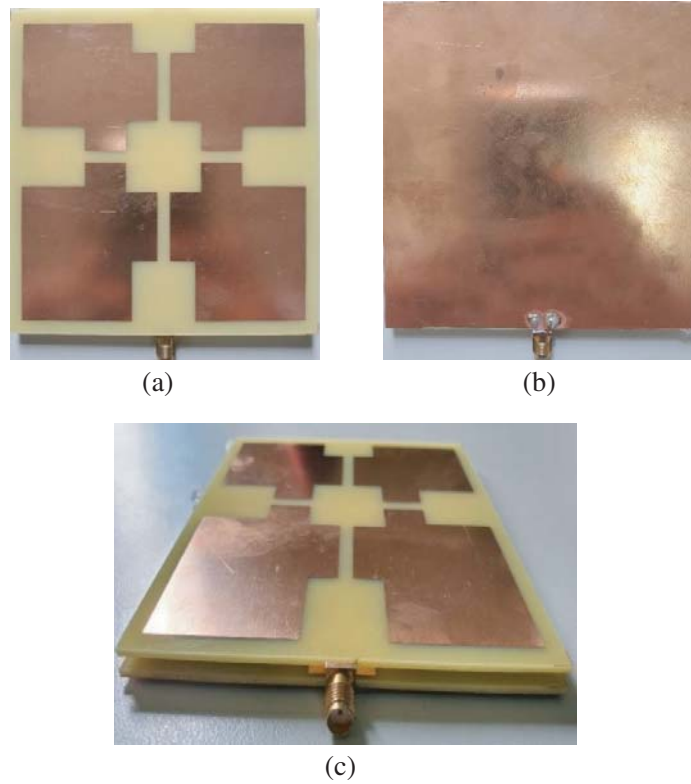


**Figure 5.** Fabricated prototype of proposed antenna. (a) Top view. (b) Back view. (c) Bird eye view.

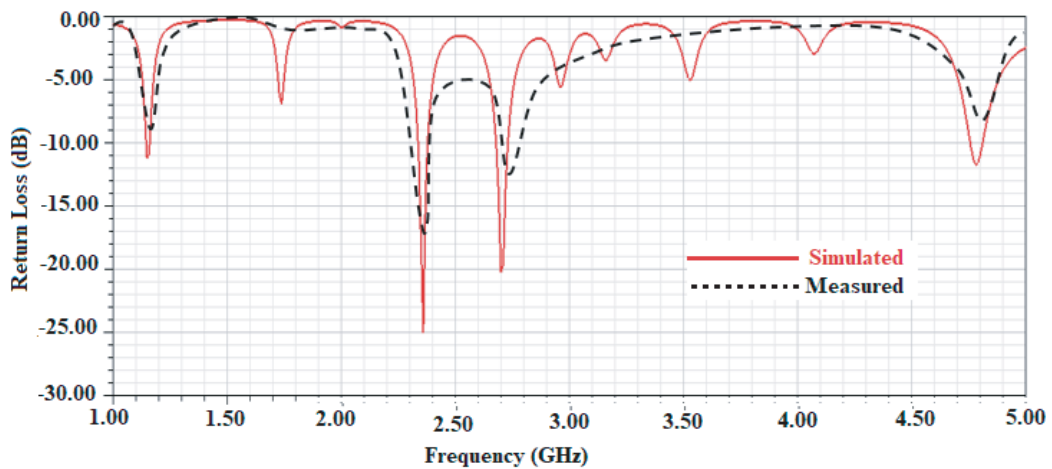


**Figure 6.** Return loss (simulated against measured).

1.40, and 1.56, respectively. These values are preferred as they are below 2.

Figure 10 depicts an E-field distribution in the main patch. This distribution is shown at 1.13 GHz, 2.47 GHz, and 2.74 GHz frequencies, respectively. An important observation could be noticed that optimum distribution is at the microstrip feedline and edges of patch geometry. The distribution is more at the edges due to discontinuity.

Similarly, Figure 11 shows an E-field distribution in the secondary patch. The distribution is shown at 1.13 GHz, 2.47 GHz, and 2.74 GHz frequencies. The secondary patch has not been excited directly by any source; however, it is coupled with the main patch and gets excited.

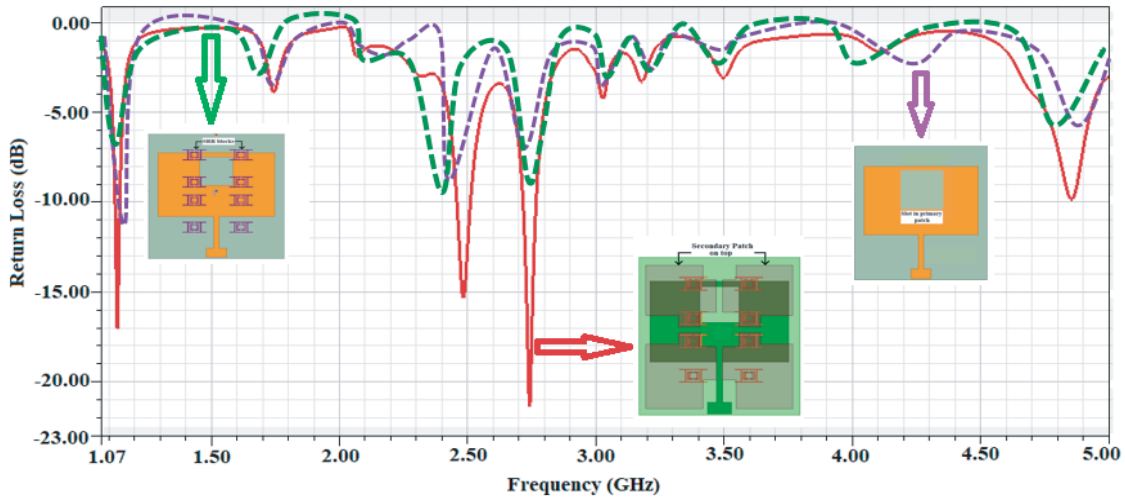


Figure 7. Return loss comparison after each iteration.

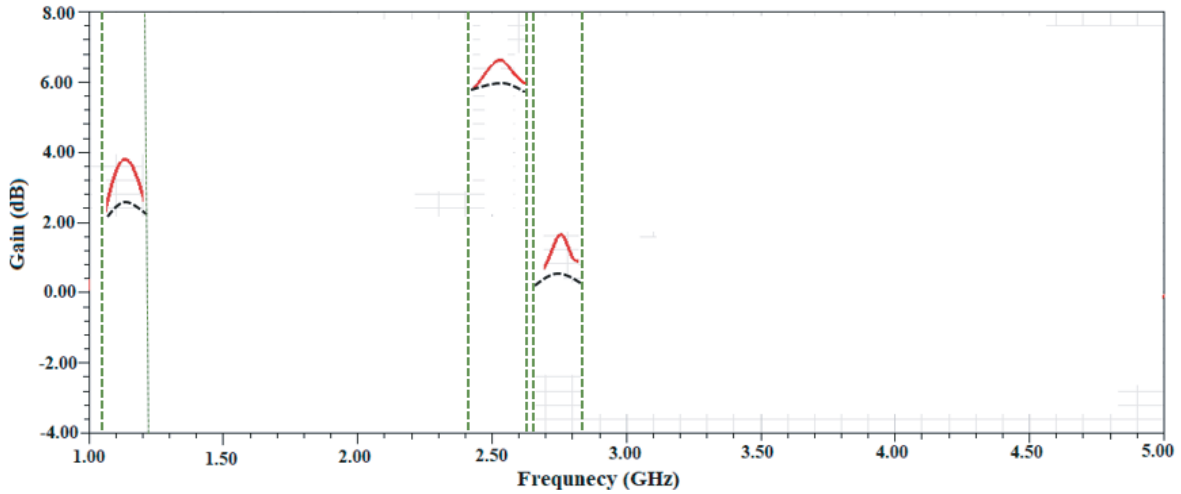


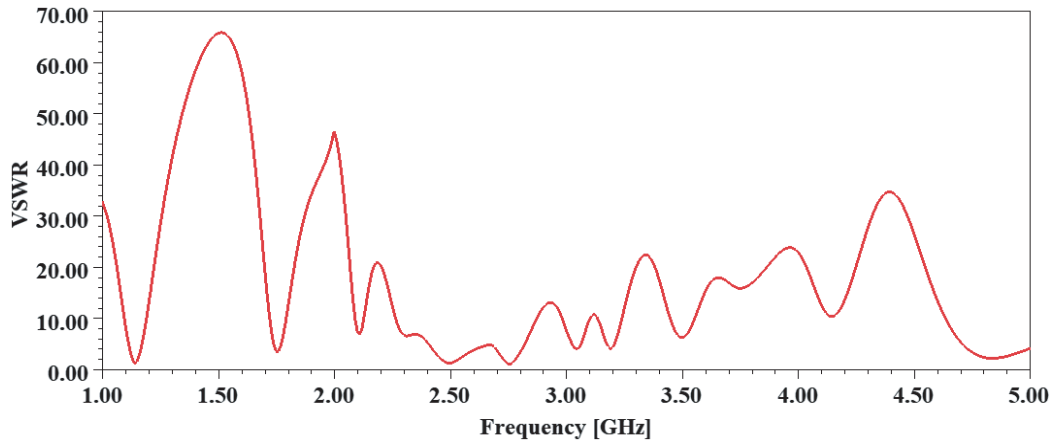
Figure 8. Gain vs frequency (simulated and measured).

Table 2 shows the comparison between simulated and measured results for return loss and impedance bandwidth at target frequencies. A minor difference could be observed between simulated and measured results due to structure complexity of the antenna.

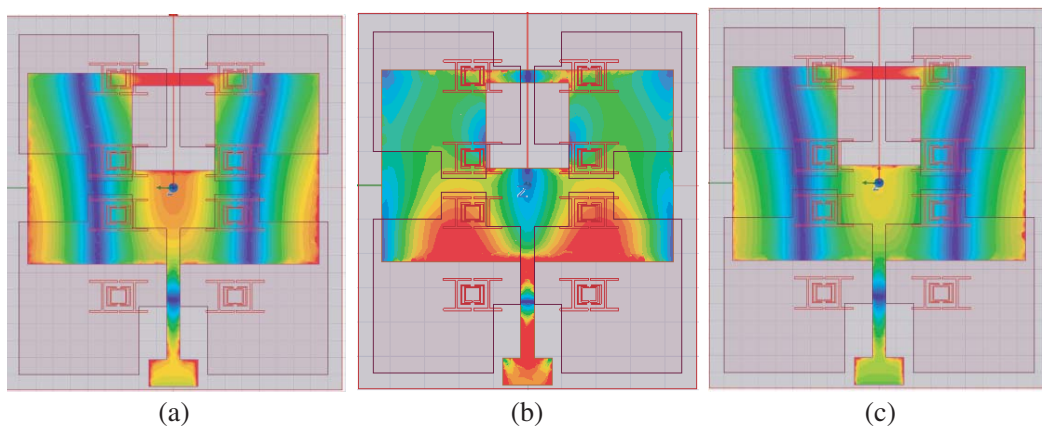
The E-field and H-field radiation patterns were measured in an anechoic chamber as illustrated in Figure 12. The size of the anechoic chamber is  $3\text{ m} \times 3\text{ m} \times 3\text{ m}$ . This chamber is suitable due to electrical compactness of the structure. Figures 13 and 14 represent the E-field and H-field radiation

Table 2. Comparison of antenna parameters at resonance frequencies.

Parameter	Reflection Coefficient (dB)		Impedance bandwidth (%)	
	Simulated	Measured	Simulated	Measured
Resonance frequencies (GHz)				
1.13	-17.33	-16.12	2.10	1.80
2.47	-15.05	-13.05	2.81	2.65
2.70	-23.05	-19.20	2.09	1.99



**Figure 9.** VSWR vs frequency.



**Figure 10.** E-field distribution in primary patch at (a) 1.13 GHz, (b) 2.47 GHz, and (c) 2.74 GHz frequencies.

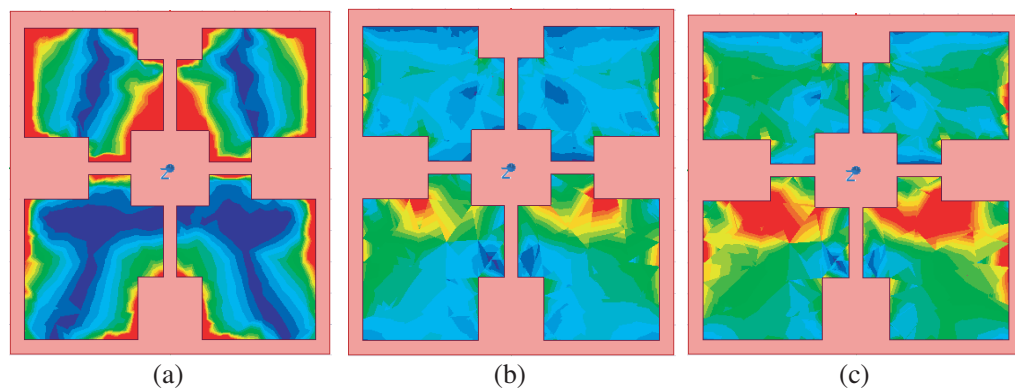


**Figure 11.** E-field distribution in secondary patch at (a) 1.13 GHz, (b) 2.47 GHz, and (c) 2.74 GHz frequencies.

patterns for 2.13 GHz, 2.47 GHz, and 2.74 GHz frequencies, respectively.

Table 3 gives the comparison of proposed antenna parameters with other important antenna models available in the literature. The comparison based on physical size, gain, and bandwidth for given substrate material is presented.

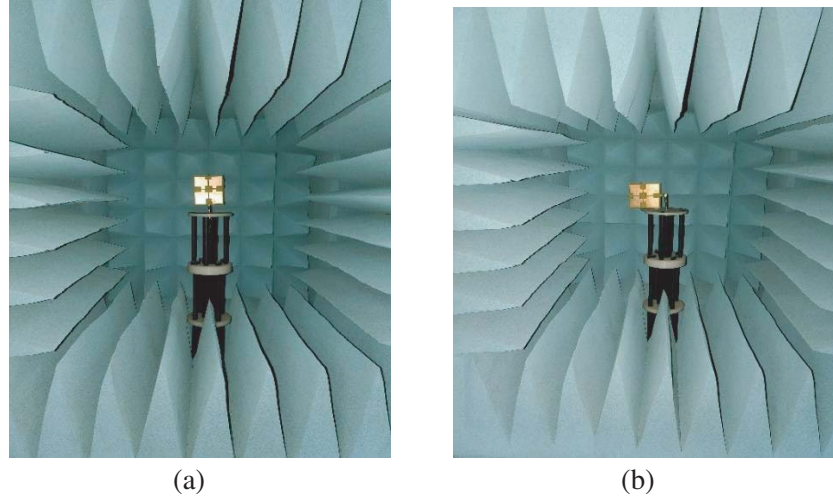


**Figure 12.** Antenna measurement in anechoic chamber. (a) *E*-plane. (b) *H*-plane.

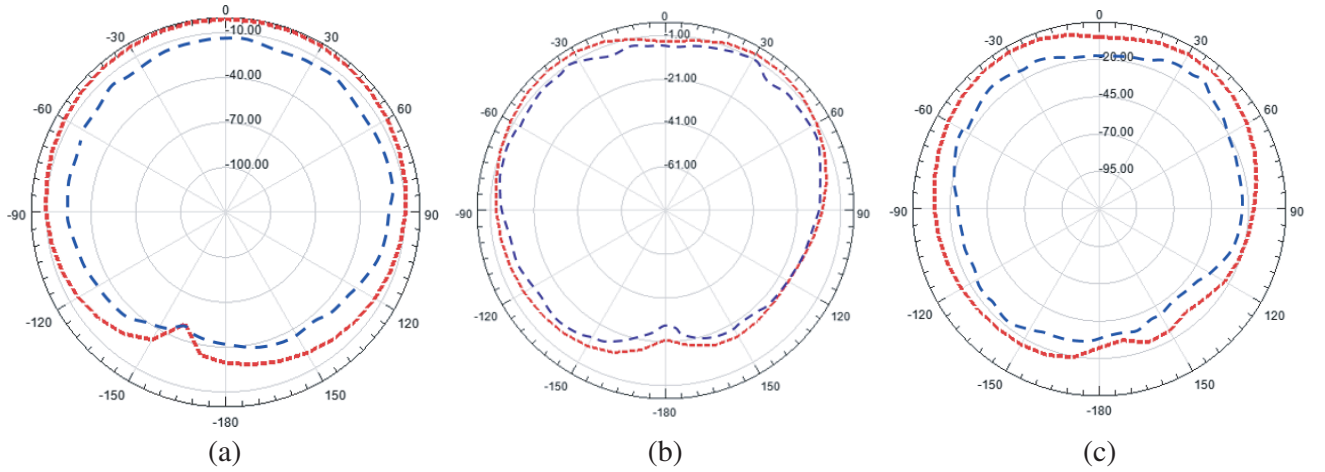


**Figure 13.** E-field radiation pattern for 2.13 GHz, 2.47 GHz and 2.74 GHz frequencies.

**Table 3.** Comparison of proposed structure with other relevant designs.

Reference	Frequency bands (GHz)	Gain (dBi)	Bandwidth (%)	Antenna dimensions (mm)	Substrate material
[5]	15.56, 20.41	1.87, 3.87	6.82, 5.55	20 × 20	Duroid 5870
[7]	1.69, 1.93, 2.20	1.08, 1.82, 2.93	4.24, 3.11, 12.73	40 × 50	FR4-epoxy
[8]	2.5, 3.5, 5.5	2, 2.23, 2.58	3.23, 4.22, 7.82	27.5 × 20	Taconic
[9]	2.4, 3.5, 5.2	-1, 1, 4	13, 17, 16	30 × 40	Rogers TMM3
[11]	2.4, 5.2, 5.8	1.53, 2.18, 2.89	18, 17, 30	32 × 32	FR4-epoxy
<b>Proposed antenna</b>	<b>1.13, 2.47, 2.74</b>	<b>3.73, 6.18, 1.35</b>	<b>2.10, 2.81, 2.09</b>	<b>35 × 45</b>	<b>FR4-epoxy</b>

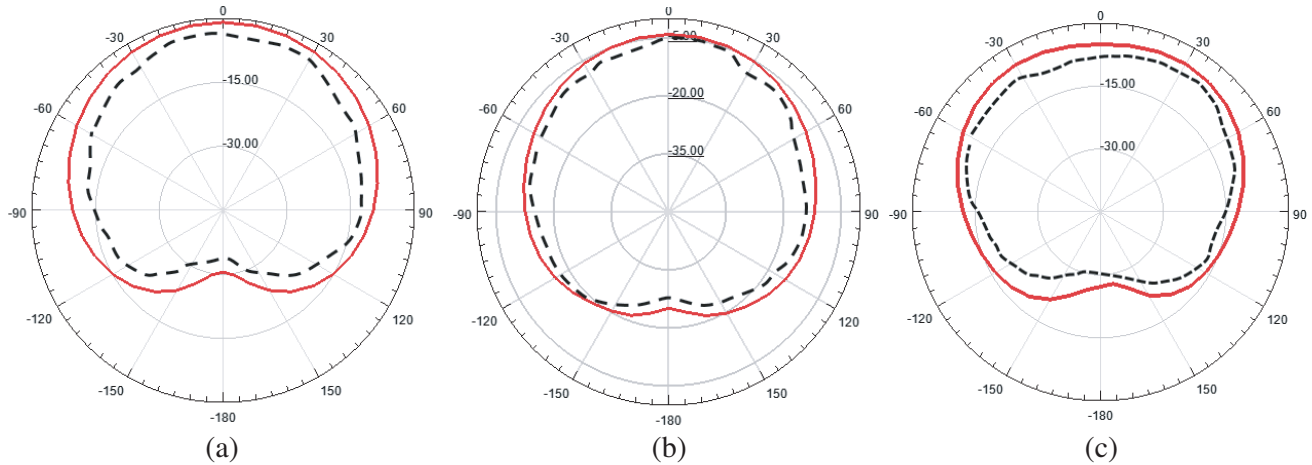


**Figure 14.** H-field radiation pattern for 2.13 GHz, 2.47 GHz and 2.74 GHz frequencies.

#### 4. CONCLUSION

The proposed multilayer antenna meets all necessary parameters for end-user applications targeted at 1.13 GHz, 2.47 GHz, and 2.74 GHz frequencies for navigation, WiFi, and satellite communication applications, respectively. Peak gains of 6.18 dBi, 3.73 dBi, and 1.75 dBi are attained at these three frequencies, respectively. The desirable performance has been attained for other antenna parameters such as return loss and radiation pattern. The antenna gain can be further increased by using low loss dielectric laminates.

#### REFERENCES

1. Pendry, J. B., A. J. Holden, D. J. Robbins, and W. J. Stewart, "Magnetism from conductors and enhanced nonlinear phenomena," *IEEE Trans. Microw. Theory Tech.*, Vol. 47, No. 11, 2075–2084, 1999.
2. Ntaikos, D. K., N. K. Bourgis, and T. V. Yioultis, "Metamaterial-based electrically small multiband planar monopole antennas," *IEEE Antennas Wirel. Propag. Lett.*, Vol. 10, 963–966, 2011.
3. Upadhyaya, T. K., S. P. Kosta, R. Jyoti, and M. Palandöken, "Novel stacked  $\mu$ -negative material-loaded antenna for satellite applications," *International Journal of Microwave and Wireless Technologies*, Vol. 8, No. 2, 229, 2016.
4. Upadhyaya, T. K., S. P. Kosta, R. Jyoti, and M. Palandoken, "Negative refractive index material-inspired 90-deg electrically tilted ultra wideband resonator," *Optical Engineering*, Vol. 53, No. 10, 107104, 2014.
5. Islam, M. M., M. T. Islam, and M. R. Faruque, "Dual-band operation of a microstrip patch antenna on a Duroid 5870 substrate for Ku- and K-bands," *Scientific World Journal*, Vol. 2013, 378420, 2013.
6. Patel, U. and T. K. Upadhyaya, "Design and analysis of compact  $\mu$ -negative material loaded wideband electrically compact antenna for WLAN/WiMAX applications," *Progress In Electromagnetics Research M*, Vol. 79, 11–22, 2019.
7. Sarkar, D., K. Saurav, and K. V. Srivastava, "Multi-band microstrip-fed slot antenna loaded with split-ring resonator," *Electron. Lett.*, Vol. 50, 1498–1500, 2014.
8. Wan, Y.-T., D. Yu, F.-S. Zhang, and F. Zhang, "Miniature multi-band monopole antenna using spiral ring resonators for radiation pattern characteristics improvement," *Electron. Lett.*, Vol. 49, 382–384, 2013.

9. Basaran, S. C., U. Olgun, and K. Sertel, "Multiband monopole antenna with complementary splitting resonators for WLAN and WiMAX applications," *Electron. Lett.*, Vol. 49, 636–638, 2013.
10. Patel, R. H., A. H. Desai, and T. Upadhyaya, "Design of H-shape X-band application electrically small antenna," *International Journal of Electrical Electronics and Data Communication (IJEEDC)*, Vol. 3, 1–4, 2015.
11. Sim, C. Y. D., H. D. Chen, K. C. Chiu, and C. H. Chao, "Coplanar waveguide fed slot antenna for wireless local area network/worldwide interoperability for microwave access applications," *IET Microw. Antenna Propag.*, Vol. 6, No. 14, 1529–1535, 2012.
12. Xu, H. X., G. M. Wang, and M. Q. Qi, "A miniaturized triple-band metamaterial antenna with radiation pattern selectivity and polarization diversity," *Progress In Electromagnetics Research*, Vol. 137, 275–292, 2013.
13. Pan, C. Y., T. S. Horng, W. S. Chen, and C. H. Huang, "Dual wideband printed monopole antenna for WLAN/WiMAX applications," *IEEE Antennas Wirel. Propag. Lett.*, Vol. 6, 149–151, 2007.
14. Xu, H. X., G. M. Wang, M. Q. Qi, C. X. Zhang, J. G. Liang, J. Q. Gong, et al., "Analysis and design of two-dimensional resonant-type composite right/left-handed transmission lines with compact gain-enhanced resonant antennas," *IEEE Trans. Antennas Propag.*, Vol. 61, No. 2, 735–747, 2013.
15. Xu, H. X., G. M. Wang, Y. Y. Lv, M. Q. Qi, X. Gao, and S. Ge, "Multifrequency monopole antennas by loading metamaterial transmission lines with dual-shunt branch circuit," *Progress In Electromagnetics Research*, Vol. 137, 703–725, 2013.
16. Xu, H. X., G. M. Wang, M. Q. Qi, and T. Cai, "Compact fractal left-handed structures for improved cross-polarization radiation pattern," *IEEE Trans. Antennas Propag.*, Vol. 62, No. 2, 546–554, 2014.
17. Li, J., Y. Cheng, Y. Nie, and R. Gong, "Metamaterial extends microstrip antenna," *Microwaves RF*, Vol. 52, 69–73, 2013.
18. Hamad, E. K. I. and A. Abdelaziz, "Performance of a metamaterial-based  $1 \times 2$  microstrip patch antenna array for wireless communications examined by characteristic mode analysis," *Radioengineering*, Vol. 28, No. 4, 681, 2019.
19. Hamad, E. K. I. and A. Abdelaziz, "Metamaterial superstrate microstrip patch antenna for 5G wireless communication based on the theory of characteristic modes," *Journal of Electrical Engineering*, Vol. 70, No. 3, 187–197, 2019.
20. Kaur, H. and A. Sharma, "Microstrip patch antennas using metamaterials: A review," *International Journal of Electronics, Electrical and Computational System*, Vol. 6, No. 6, 130–133, 2017.
21. Smith, D. R., S. Schultz, P. Markos, and C. M. Soukoulis, "Determination of negative permittivity and permeability of metamaterials from reflection and transmission coefficients," *Phys. Rev. B*, Vol. 65, 195104–195109, 2002.
22. Singh, H. P. and R. Y. Kumar, "Design and simulation of rectangular microstrip patch antenna loaded with metamaterial structure," *Electric Electron. Tech. Open Acc. J.*, Vol. 1, No. 2, 00012, 2017.
23. Gangwar, K., P., R. P. S. Gangwar and R. Verma, "Multiband microstrip patch antenna using metamaterial structure," *2nd International Conference on Emerging Trends in Technology and Applied Sciences (ICETTAS'15)*, 2018.
24. Islam, M. R., A. A. Alsaleh Adel, A. W. N. Mimi, M. Sarah Yasmin, and F. A. M. Norun, "Design of dual band microstrip patch antenna using metamaterial," *IOP Conference Series: Materials Science and Engineering*, Vol. 260, No. 1, 012037, IOP Publishing, 2017.
25. Li, L.-W., Y.-N. Li, T.-S. Yeo, J. R. Mosig, and O. J. F. Martin, "A broadband and high-gain metamaterial microstrip antenna," *Applied Physics Letters*, Vol. 96, No. 6, 164101, April 2010.
26. Palandoken, M., A. Grede, and H. Henke, "Broadband microstrip antenna with lefthanded metamaterials," *IEEE Trans. Antennas Propag.*, Vol. 57, 331–338, 2009.
27. Lee, C. J., K. M. K. H. Leong, and T. Itoh, "Composite right/left-handed transmission line based compact resonant antennas for RF module integration," *IEEE Trans. Antennas Propag.*, Vol. 54, 2283–2291, 2006.

28. Iizuka, H. and P. S. Hall, "Left-handed dipole antennas and their implementations," *IEEE Trans. Antennas Propag.*, Vol. 55, 1246–1253, 2007.
29. Vahora, A. and K. Pandya, "Implementation of cylindrical dielectric resonator antenna array for Wi-Fi/wireless LAN/satellite applications," *Progress In Electromagnetics Research M*, Vol. 90, 157–166, 2020.
30. Pimpalgaonkar, P. R., T. K. Upadhyaya, K. Pandya, M. R. Chaurasia, and B. T. Raval, "A review on dielectric resonator antenna," *1st International Conference on Automation in Industries (ICAI)*, 106–109, June 2016.
31. Vahora, A. and K. Pandya, "Triple band dielectric resonator antenna array using power divider network technique for GPS navigation/bluetooth/satellite applications," *International Journal of Microwave and Optical Technology*, Vol. 15, 369–378, July 2020.
32. Vahora, A. and K. Pandya, "Microstrip feed two elements pentagon dielectric resonator antenna array," *2019 International Conference on Innovative Trends and Advances in Engineering and Technology (ICITAET)*, 22–25, IEEE, 2019.
33. Pimpalgaonkar, P. R., M. R. Chaurasia, B. T. Raval, T. K. Upadhyaya, and K. Pandya, "Design of rectangular and hemispherical dielectric resonator antenna," *2016 International Conference on Communication and Signal Processing (ICCSP)*, 1430–1433, IEEE, 2016.
34. Patel, A., Y. Kosta, N. Chhasatia, and K. Pandya, "Multiple band waveguide based microwave resonator," *IEEE International Conference on Advances in Engineering, Science and Management (ICAESM-2012)*, 84–87, IEEE, March 2012.